Available online at www.sciencedirect.com

SciVerse ScienceDirect

Ceramics International 39 (2013) S729–S732

CERAMICS INTERNATIONAL

www.elsevier.com/locate/ceramint

Bipolar resistive switching properties in transparent vanadium oxide resistive random access memory

Fann-Wei Yang[a], Kai-Huang Chen[b,*], Chien-Min Cheng[a], Feng-Yi Su[a]

[a]*Department of Electronic Engineering, Southern Taiwan University of Science and Technology-No. 1, Nan-Tai Street, Yungkang District, Tainan City 710, Taiwan, ROC*

[b]*Department of Electronics Engineering and Computer Science, Tung-Fang Design University, Kaohsiung City 829, Taiwan, ROC*

Available online 17 October 2012

Abstract

The bipolar switching and electrical conduction properties in transparent vanadium oxide (VO) resistance random access memory device were investigated in this study. The as-deposited VO thin films were deposited onto transparent indium tin oxide (ITO) substrate for the possible application in the structure of system on panel (SOP) devices. The transmittance of as-deposited VO thin films within the UV–vis spectrum in the wavelength range of 300–1100 nm was obtained. In addition, the Al/VO/ITO device shows reliable bipolar switching behaviors. The on/off ratio and biopolar switching cycling of two stable states for resistance random access memory device were found. We suggested that the current–voltage characteristics were governed by the space charge limit conduction (SCLC) transport models mechanism in low and high voltage regions.

Keywords: C. Electrical properties; C. Electrical conductivity; E. Capacitors; E. Functional applications

1. Introduction

Various functional thin films were widely focused on the applications in non-volatile random access memory (NvRAM), for example smart memory cards and portable electrical devices which utilize excellent memory characteristics such as high storage capacity, long retention cycles, low electric consumption, non-volatility, and high speed readout. Besides, the various non-volatile random access memory devices, like ferroelectric random access memory (FeRAM), magnetron memory (MRAM), resistance random access memory (RRAM), and flash memory were widely discussed and investigated [1–10]; however, RRAMs are attractive in the sunrise memory device applications. In addition, systems on panel (SOP) technology is also widely investigated and the integrated electronic devices on transparent conductive thin film will be important in the future. High quality and reliable transparent conductive thin films on glass substrate for RRAM cell were also developed [1,9]. The objective of this work is to study the possible applications of vanadium oxide (VO) thin films deposited onto ITO/glass substrate as transparent RRAM. The bipolar resistive switching properties of VO thin films were well developed and investigated in the metal–insulator–metal (MIM) structure for application in memory devices. We show that as-deposited VO thin film is a candidate for fabrication of the memory devices. In addition, the leakage current density, current transport mechanism, and the current ratio of VO thin films were fabricated using rf magnetron sputtering and were characterized.

2. Experimental details

The VO thin films were deposited onto ITO/glass substrate by the rf magnetron sputtering method under the optimal deposition parameters such as the rf power of 110 W, chamber pressure of 10 mTorr, and oxygen concentration of 40%. The XRD patterns of the VO thin films were recorded to determine their crystallographic structure in the 2θ-degree range of 20–60° using SIEMENS D5000. To complete the MIM structure, the VO target was placed 5–8 cm away from the ITO/glass substrate. An array of

*Corresponding author. Tel.: +886 7 6939626; fax: +886 7 6933406.
E-mail address: d9131802@gmail.com (K.-H. Chen).

0272-8842/$ - see front matter
http://dx.doi.org/10.1016/j.ceramint.2012.10.170

circular top contacts with a diameter of 0.1 cm was formed by depositing an Al film with 500 nm thickness through a metal mask by thermal evaporation in a vacuum system operating at 1×10^{-5} Torr. The MIM devices are schematically shown in Fig. 1. The current versus applied voltage (I–V) properties of VO thin films were measured by a semiconductor parameter analyzer (HP 4156).

3. Results and discussion

Fig. 2 shows the X-ray diffraction patterns of the as-deposited VO thin films for 60% oxygen concentration on ITO substrate prepared with sintering at different temperatures. From the XRD patterns, we found that the VO thin films exhibited polycrystalline structure. In addition, the (110), (222), and (400) peaks were observed in the XRD pattern.

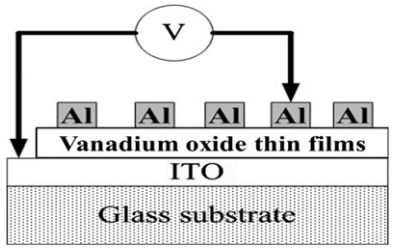

Fig. 1. Metal–insulator–metal (MIM) structure using as-deposited VO thin films.

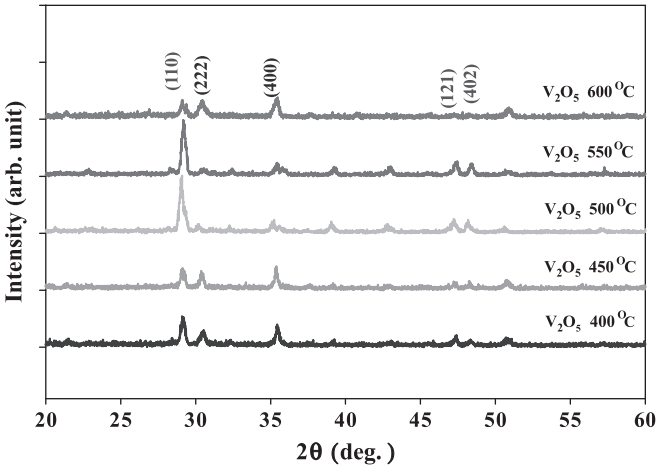

Fig. 2. X-ray diffraction patterns of the as-deposited VO thin films on ITO substrate for different sintering temperatures.

The intensity of the (110) peak of the thin films increases linearly as the sintering temperature increases from 400 to 550 °C. The intensity of the (110) peak of the as-deposited thin films decreases at sintering temperatures from 550 to 600 °C. As shown in Fig. 2, the (110) preferred phase and the smallest full-width-half-maximum (FWHM) value were exhibited by the as-deposited VO thin film with sintering at a temperature of 550 °C. The polycrystalline structure of the as-deposited VO thin film was optimal at 550 °C sintering temperature.

The thickness of as-deposited vanadium oxide thin films for different sintering temperatures was determined by SEM morphology. As the oxygen concentration increases from 0% to 60%, the thickness of as-deposited vanadium oxide thin films decreases linearly. In addition, the deposition rate of as-deposited VO thin films with 60% oxygen concentration was 2.62 nm/min. The decrease in the deposition rate and thickness of as-depoisted VO thin films might be affected by the decrease in Ar/O_2 ratio.

The Ar/O_2 ratio was adjusted using argon gas to generate the plasma on the surface of the as-depoisted VO ceramic target during sputtering. Fig. 3 shows the surface morphology for the as-deposited and 500 °C sintered VO thin films. We found that the grain sizes of 500 °C sintered VO thin films were larger than the others. Fig. 4 shows the current versus applied voltage (I–V) properties of VO thin films for various oxygen concentrations. After the starting process, the device reached a low resistance state (LRS) and a high resistance state (HRS). By sweeping the bias to negative over the reset voltage, a gradual decrease of current was presented to switch the cells from LRS to HRS (reset process). Additionally, the cell turns back to LRS on applying a larger positive bias than the set voltage (set process).

All of the VO thin films exhibit a bipolar behavior. The I–V properties of as-deposited VO thin films of 60% oxygen concentration were about 1×10^{-4} A/cm^2 under an applied electrical voltage of 0.1 V. During the rf sputtering deposition process, oxygen vacancies appeared in the as-deposited VO thin films. The defects and oxygen

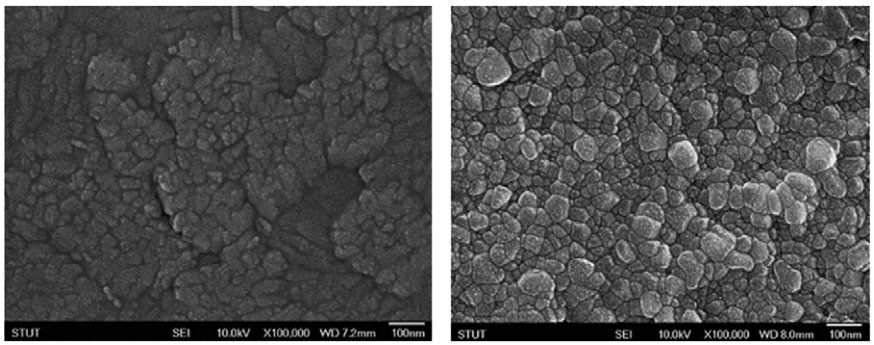

Fig. 3. Surface morphology for (a) as-deposited and (b) 500 °C sintered VO thin films.

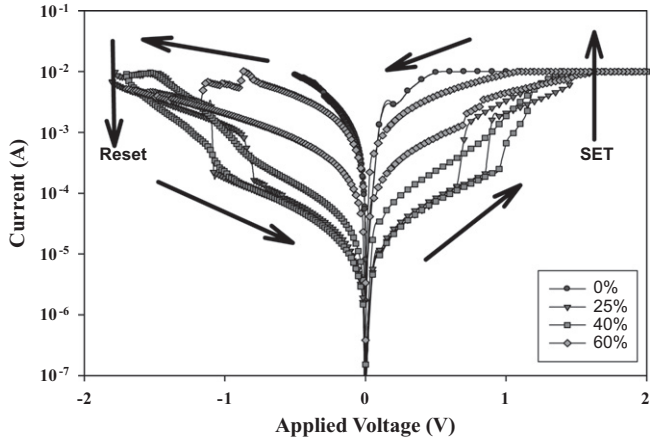

Fig. 4. Typical *I–V* characteristics of VO thin films for different oxygen concentrations.

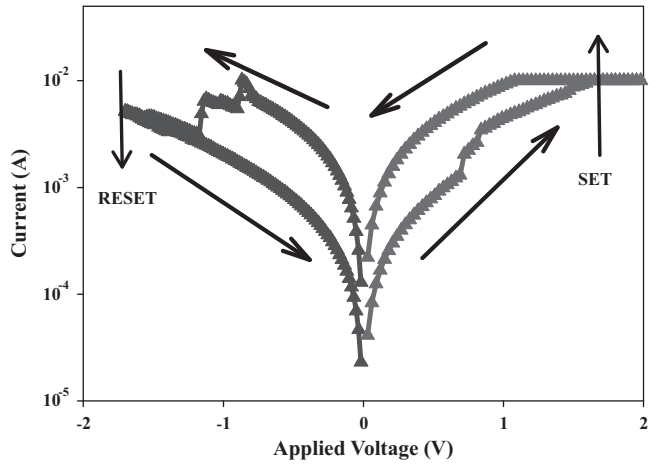

Fig. 5. Typical *I–V* characteristics of VO thin films for the 60% oxygen concentration.

vacancies of as-deposited VO thin films were filled and compensated for different extents at different oxygen concentrations. In addition, the smallest leakage current density of as-deposited VO thin films was obtained at an oxygen concentration of 40%. As shown in Fig. 4, the high leakage current density and thin films of as-deposited VO thin films for 60% oxygen concentration were attributed to a low argon sputtering gas concentration.

Fig. 5 shows the current versus applied voltage (*I–V*) properties of the transparent resistance random access memory (RRAM) devices on ITO electrode using the VO thin films, which exhibit the characteristic bipolar behavior. Therefore, the *I–V* of as-deposited VO thin films of 60% oxygen concentration has exhibited large on/off ratio memory property.

Fig. 6 shows the current versus applied voltage (*I–V*) properties of the as-deposited VO thin films for 60% oxygen concentration on ITO substrate prepared by sintering at different temperatures. From the *I–V* properties, we found that the VO thin films show better non-volatile resistance memory properties.

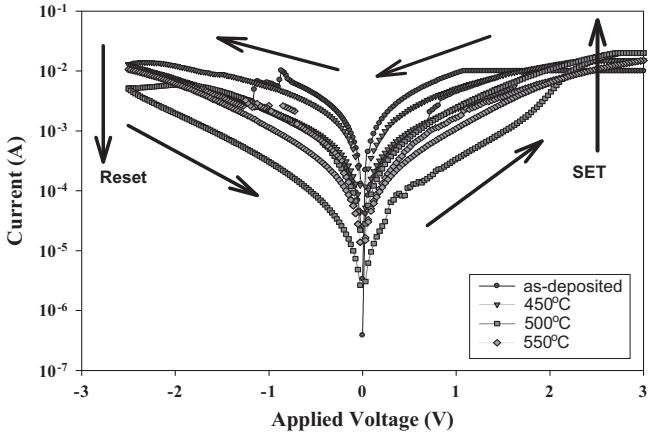

Fig. 6. Typical *I–V* characteristics of the as-deposited VO thin films for different sintering temperatures.

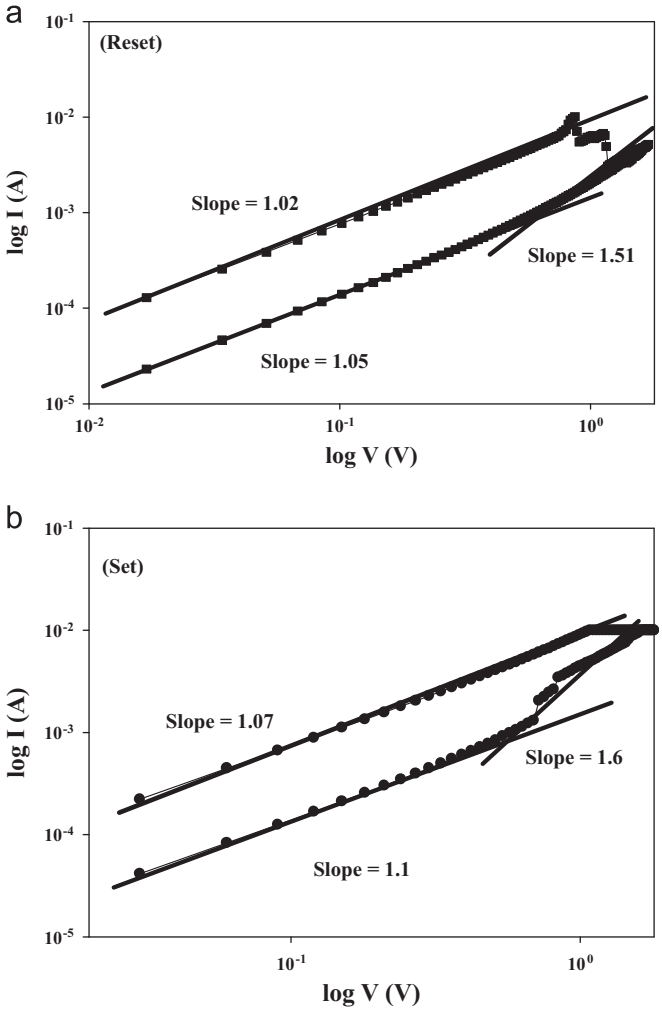

Fig. 7. (a) The log–log plot of *I–V* in the reset and (b) in the set state of the 500 °C sintered VO thin films for different sintering temperatures.

In addition, the transport current of the VO thin films decreases linearly as the sintering temperature increases from 450 to 500 °C. The transport current of the as-deposited VO

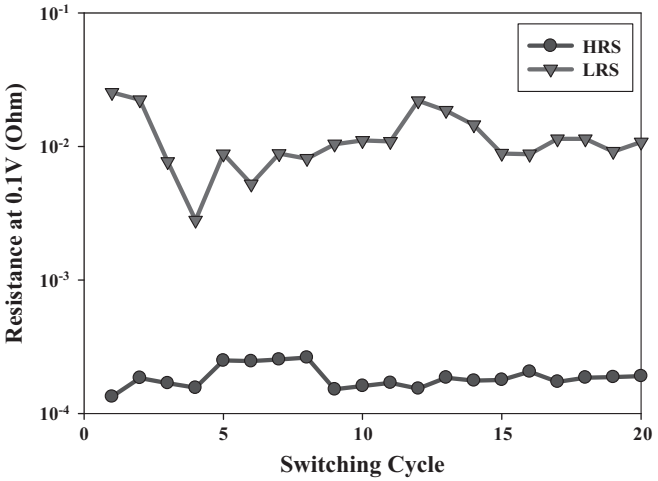

Fig. 8. Switching cycle of the transparent resistance random access memory (RRAM) devices at room temperature measured at 0.5 V.

thin films increases at sintering temperature from 500 to 550 °C. We found that the as-deposited VO thin films prepared by sintering at 500 °C temperature exhibited the largest on/off ratio resistance property.

Fig. 7(a) shows the *J–E* characteristics of VO thin films for the RRAM devices in terms of log *I* as vertical axis and applied electrical field log *V* as horizontal axis. The fitting curves were straight in this figure, and the log *I* versus log *V* curves obey the Child law model. For slope = 1, the VO thin films at 500 °C sintering temperature exhibit the Ohmic conduction for positive applied voltage of 0.1–2.5 V. For slope = 2, the 500 °C sintered VO thin films exhibit Child's law in a high applied voltage and it was at the trap center region. The result has proved that it was caused by the carriers filling the traps and defects in the 500 °C sintered VO thin films. The log *I* versus log *V* curves of the RRAM devices for negative bias are shown in Fig. 7(b). The 500 °C sintered VO thin films for slope = 1 also exhibit the Ohmic conduction for applied voltage of 0.1–2.5 V. The switching cycles of reliability and retention characteristics for the VO RRAM devices were measured and are shown in Fig. 8. There was a slight fluctuation of resistance in the HRS and LRS states, and the stable bipolar switching property was observed during the 20 cycles. The results show a remarkable reliable performance of the RRAM devices for non-volatile memory applications.

The transmittance of VO thin films within the UV–vis spectrum in the wavelength range of 300–1100 nm at different oxygen concentrations was obtained. The transmittance in the visible range, 400–700 nm, of as-deposited VO thin films was determined, and the maximum transparency range was 92–97%. As the oxygen concentration increases, the maximum transparency of the 60% oxygen as-deposited VO thin films increases.

4. Conclusion

In conclusion, the VO thin films were deposited on ITO/glass substrate using the rf magnetron sputtering method. All the VO thin films developed in this study exhibited transparency within the visible range. In addition, the transparent RRAM devices exhibited the bipolar behavior. The conduction behavior of the sintered VO thin films exhibits the Ohmic conduction for applied voltage of 0.1–2.5 V. The as-deposited VO thin films exhibited the Child's law in high applied voltage and it was at the trap center region. From these results, we conclude that the VO thin films will be an excellent candidate for the RRAM memory devices or other devices in the application of system on panel (SOP) structures.

Acknowledgments

We acknowledge the financial support of the National Science Council of the Republic of China (NSC 100-2221-E-272-003).

References

[1] K.H. Chen, Y.C. Chen, C.F. Yang, T.C. Chang, Fabrication and characteristics of $Ba(Zr_{0.1}Ti_{0.9})O_3$ thin films on glass substrate, Journal of Physics and Chemistry of Solids 69 (2008) 461–464.
[2] C.F. Yang, K.H. Chen, Y.C. Chen, T.C. Chang, Fabrication of one-transistor–capacitor structure of nonvolatile TFT ferroelectric RAM devices using $Ba(Zr_{0.1}Ti_{0.9})O_3$ gated oxide film, IEEE Ultrasonic, Ferroelectric and Frequency Control 54 (2007) 1726–1730.
[3] C.F. Yang, K.H. Chen, Y.C. Chen, T.C. Chang, Physical and electrical characteristics of $Ba(Zr_{0.1}Ti_{0.9})O_3$ thin films under oxygen plasma treatment for applications in non-volatile memory devices, Applied Physics A 90 (2008) 329–331.
[4] K.H. Chen, Y.C. Chen, Z.S. Chen, C.F. Yang, T.C. Chang, Temperature and frequency dependence of the ferroelectric characteristics of $BaTiO_3$ thin films for nonvolatile memory applications, Applied Physics A 89 (2007) 533–536.
[5] M.C. Kuan, C.M. Cheng, K.H. Chen, C.C. Lin, Influence of lithium and potassium doping on structure and electrical characteristics of $Li_x(K_yNa_{1-y})_{-x}(Nb_{0.9}Ta_{0.06}Sb_{0.04})O_3$ lead-free piezoelectric ceramics, Japanese Journal of Applied Physics 51 (2012) 035801–035804.
[6] K.H. Chen, C.M. Cheng, C.C. Shih, J.H. Tsai, The influence of lanthanum doping on the physical and electrical properties of BTV ferroelectric thin films, Applied Physics A 103 (2011) 1173–1177.
[7] C.M. Cheng, M.C. Kuan, K.H. Chen, J.H. Tsai, Electric aging behavior of lead-free $Li_{0.06}(K_{0.48}Na_{0.52})_{0.94}(Nb_{0.86}Ta_{0.08}Sb_{0.06})O_3$ piezoelectric ceramics improved by pre-calcined method, Ceramics International 38 (2012) S335–S338.
[8] K.H. Chen, C.H. Chang, C.M. Cheng, C.F. Yang, Large memory window in the vanadium doped $Bi_4Ti_3O_{12}$ thin films, Applied Physics A 97 (2009) 919–923.
[9] K.H. Chen, T.C. Chang, G.C. Chang, Y.E. Hsu, Y.C. Chen, H.Q. Xu, Low temperature improvement method on characteristics of $Ba(Zr_{0.1}Ti_{0.9})O_3$ thin films deposited on indium tin oxide/glass substrates, Applied Physics A 99 (2010) 291–295.
[10] C.M. Cheng, K.H. Chen, J.H. Tsai, C.L. Wu, Solution based fabrication and electrical properties of $CaBi_4Ti_4O_{15}$ thin films, Ceramics International 38 (2012) S87–S90.